

University of Texas Rio Grande Valley

ScholarWorks @ UTRGV

---

Mathematical and Statistical Sciences Faculty  
Publications and Presentations

College of Sciences

---

2013

## The Two-Phase Arterial Blood Flow with or without a Catheter and in the Presence of a Single or Multi Stenosis

Ani E. Garcia

Daniel N. Riahi

*The University of Texas Rio Grande Valley*

Follow this and additional works at: [https://scholarworks.utrgv.edu/mss\\_fac](https://scholarworks.utrgv.edu/mss_fac)



Part of the [Mathematics Commons](#), and the [Medicine and Health Sciences Commons](#)

---

### Recommended Citation

Garcia, A. E., & Riahi, D. N. (2013). The Two-Phase Arterial Blood Flow with or without a Catheter and in the Presence of a Single or Multi Stenosis. *Applications and Applied Mathematics: An International Journal*, 8(2), 17.

This Article is brought to you for free and open access by the College of Sciences at ScholarWorks @ UTRGV. It has been accepted for inclusion in Mathematical and Statistical Sciences Faculty Publications and Presentations by an authorized administrator of ScholarWorks @ UTRGV. For more information, please contact [justin.white@utrgv.edu](mailto:justin.white@utrgv.edu), [william.flores01@utrgv.edu](mailto:william.flores01@utrgv.edu).



## The Two-Phase Arterial Blood Flow with or without a Catheter and in the Presence of a Single or Multi Stenosis

Ani E. Garcia and Daniel N. Riahi\*

Department of Mathematics  
University of Texas-Pan American  
1201 West University Drive,  
Edinburg, Texas 78539-2999, USA  
[driahi@utpa.edu](mailto:driahi@utpa.edu)

Received: February 7, 2013; Accepted: August 18, 2013

\*Corresponding Author

### Abstract

We consider the problem of blood flow in an artery with or without a catheter and in the presence of single or multi stenosis whose shape is based on the available experimental data for the stenosis in a human's artery. The presence of stenosis in the artery, which locally narrows portion of the artery, can be a result of fatty materials such as cholesterol in the blood. The use of catheter is important as a standard tool for diagnosis and treatment in patients whose blood flow passage in the artery is affected adversely by the presence of the stenosis within the artery. The blood flow in the arterial tube is represented by a two-phase model composing a suspension of red cells in plasma. The governing equations for both fluid (plasma) and particles (red cells) are solved subject to reasonable modeling and approximations. The important quantities such as blood velocity, blood pressure gradient, impedance (blood flow resistance), wall shear stress and its surface integrated force are computed in the presence or absence of the catheter, and, in particular, effects of the stenosis, size of the catheter's radius and the hematocrit due to the red cells-plasma combination of the blood flow are determined.

**Keywords:** Arterial flow, blood flow, impedance, multi stenosis, stress force

**AMS-MSC 2010 No.:** 76Z, 92B

## 1. Introduction

Diseases in the blood vessels and in the heart, such as heart attack and stroke, are the major causes of mortality worldwide. The underlying cause for these health problems is the formation of lesions referred to here as stenosis. These lesions and plaques can grow and occlude the artery and hence prevent blood supply to the distal bed. Plaques with calcium in them can also rupture and initiate the formation of blood clots (thrombus). The clots can form as emboli and occlude the smaller vessels that can also result in interruption of blood supply to distal bed. Plaques formed in coronary arteries can lead to heart attacks and clots in the cerebral circulation can result in the stroke. There are a number of risk factors in the presence of stenosis. The common sites for the formation and development of stenosis include the coronary arteries, the branching of the subclavian and common carotids in the aortic arch, the bifurcation of the common carotid to internal and external carotids especially in the carotid sinus region distal to the bifurcation, the renal arterial branching in the descending aorta and in the ileofemoral bifurcations of the descending aorta.

The common feature in the location for the development of the lesion is the presence of curvature, branching, and bifurcation present in these sites. The fluid dynamics at these sites can be anticipated to be vastly different from other segments of the arteries that are relatively straight and devoid of any branching segments. Hence, several investigators have attempted to link the fluid dynamically induced stress with the formation of stenosis in the human circulation. By assuming the artery to be circularly cylindrical in shape, Mishra (2003) discussed characteristics of blood flow in stenosed artery and the stenosis was considered to be symmetric about the axis of artery. Mishra and Panda (2005) studied the flow of blood in the stenosed artery for the Casson type fluid. Young and Tsai (1973) discussed some characteristics of the flow of blood in stented arteries.

The blood vessels carry blood from the heart to all the organs and tissues of the body including the brain, kidneys, gut, muscles, and the heart itself. Venkateswarlu and Rao (2004) studied an assumed oscillatory form of the blood flow through an indented tube in the presence of a steady single stenosis with a very simple shape. They used the so-called Einstein model for the viscosity of the blood but for variable volume flow rate and the prescribed value for the magnitude of the pressure gradient. Smali et al. (2006) did some modeling and computation of blood flow through multi-stenosis and used analytical model for the shape and structure of the multi stenosis. Srivastava et al. (2010) studied arterial blood flow through an overlapping stenosis (Mishra and Panda, 2005) by using a Casson type fluid flow. They calculated impedance and shear stress for different values of the stenosis height. Riahi et al. (2011) investigated arterial blood flow in the presence of an overlapping stenosis using a variable viscosity model due to Einstein for the blood flow.

All the investigations described above were for the cases where no catheter was inserted into the artery, but there have also been a number of studies of the blood flow systems in catheterized arteries (Kanai et al., 1970; Back, 1994; Back et al., 1996; Srivastava and Rastogi, 2010). Use of

the catheter is important and has become a standard tool for the diagnostic and treatment of medical problems due to the presence of stenosis in arteries. Transducers attached to catheters are of greater use to measure blood pressure in arteries. To reduce the adverse effect of stenosis, a catheter with a tiny balloon attached at the end is inserted in the artery; the balloon is inflated to fracture fatty deposits and widen narrowed portions in the artery. A number of studies that have been carried out so far (Mishra and Pandra, 2005; Smali et al., 2006; Riahi et al., 2011) were based on a single-phase models of the blood flow in arteries which are known to be valid for flow in large arteries but fail to provide correctly the behavior of the blood flow in narrow arteries (Srivastava and Srivastava, 1983) whose corresponding blood flows can be investigated more realistically by the two-phase flow models.

In a large number of studies that have been carried out so far by different authors for the arterial blood flow systems, some of which were listed in the previous paragraphs, the shape of the stenosis were assumed to be in the form of some mathematical functions, and a number of these studies also used the single-phase model approaches. In the present study we apply for the first time an experimentally based shape (Back et al., 1984) for the stenosis in a narrow artery (Figure 1), where the blood flow is represented by a two-phase macroscopic model so that the effects of the presence of the red cells can be taken into account more realistically. It turns out that this can have notable effects on the expressions for important quantities such as the blood pressure gradient, plasma velocity, etc. In figure 1 we provide the dimensionless shape function  $R(z)$  of the multi stenosis versus the dimensionless axial variable of an artery based on the actual data determined from the experimental values of the cross-sectional area of the artery of a human in the presence of stenosis (Back et al., 1984). Here and as in the more realistic cases, the blood flow is composed of a suspension of red cells in plasma.

## 2. Formulation and Analysis

We consider the problem of axisymmetric flow of blood in a catheterized artery in the form of a circular cylindrical annulus with the outer radius  $R_0$  (radius of the normal artery) and the inner radius  $r_1$  (radius of the catheter) and in the presence of single or multiple stenosis (figure 1) whose shape is determined from the experimentally collected data (Back et al., 1984). The artery is assumed to be sufficiently long in comparison to its radius so that the end effects can be neglected. We also examined the arterial blood flow described above in the absence of the catheter ( $r_1 = 0$ ) in order to be able to isolate the effects solely due to the presence of the catheter.

The two-phase arterial blood flow system is based on the original governing equations for the mass conservation and momentum (Batchelor, 1970) for both fluid plasma and the suspended particles (red cells) as their steady axisymmetric form in cylindrical coordinate system with axial direction along the co-axial direction of the catheterized artery are given by (Srivastava and Rastogi, 2010)

$$(1-C)\rho_f (u_f \partial u_f / \partial z + v_f \partial u_f / \partial r) = -(1-C) \partial P / \partial z + (1-C)\mu_s \nabla^2 u_f + CS' (u_p - u_f), \quad (1a)$$

$$(1-C)\rho_f (u_f \partial v_f / \partial z + v_f \partial v_f / \partial r) = -(1-C) \partial P / \partial r + (1-C)\mu_s (\nabla^2 - 1/r^2) v_f + CS' (v_p - v_f), \quad (1b)$$

$$(1/r)(\partial/\partial r)[(1-C)v_f]+(\partial/\partial z)[(1-C)u_f]=0, \quad (1c)$$

$$C\rho_p[u_p\partial u_p/\partial z+ v_p\partial u_p/\partial r]=-\partial P/\partial z+ CS'(u_f-u_p), \quad (1d)$$

$$C\rho_p[u_p\partial v_p/\partial z+ v_p\partial v_p/\partial r]=-\partial P/\partial r+ CS'(v_f-v_p), \quad (1e)$$

$$(1/r)(\partial/\partial r)(Cr v_p)+(\partial/\partial z)(Cu_p)=0. \quad (1f)$$

Here  $\nabla^2 \equiv [(1/r)(\partial/\partial r)(r\partial/\partial r)+\partial^2/\partial z^2]$  is the Laplacian operator,  $r$  ( $r_1 \leq r \leq R_0$ ) and  $z$  are the cylindrical coordinates with axial variable  $z$  along the tube axis and radial variable  $r$  along the direction perpendicular to the tube axis, subscripts “f” and “p” refer to fluid (plasma) and particle (erythrocyte) quantities, respectively,  $u$  and  $v$  are the axial and radial velocity components, respectively,  $\rho$  is density,  $P$  is pressure,  $C$  is the volume fraction density of the particles, referred to here as the hematocrit % (Srivastava and Rastogi, 2010), and the expressions for the viscosity of suspension  $\mu_s$  and the drag coefficient of interaction  $S'$  have been chosen to be (Srivastava, 1996; Srivastava and Srivastava, 2009)

$$\mu_s = \mu_0 / (1-mC), \quad m = 0.07 \exp[2.49C + (1107/T) \exp(-1.69C)], \quad (1g)$$

$$S' = 4.5(\mu_0/a_0^2) \{ [4 + 3(8C - 3C^2)^{0.5} + 3C] / (2 - 3C)^2 \}, \quad (1h)$$

where  $\mu_0$  is the plasma viscosity,  $2a_0$  is the length scale of a red cell (Srivastava and Rastogi, 2010) and  $T$  is absolute temperature measured in Kelvin. Based on the reasonable suggestion by Charm and Kurland (1974), the expression for the plasma viscosity given by (1g) is accurate up to 60% hematocrit ( $C = 0.6$ ), and the expression (1h) was derived first by Tam (1969) representing classical Stokes drag valid for small particle Reynolds number.

We consider the governing equations (1a-h) for the blood flow in the axisymmetric form and use cylindrical coordinate system with  $r$  as the radial variable,  $z$  as the axial variable and with the  $z$ -axis along the axis of cylindrical artery tube, where a catheter in the form of a tube with small radius and co-axial with the cylindrical artery is placed in the artery. We also consider the same blood flow system but in the absence of the catheter by setting the value of the catheter's radius equal to zero. The inside boundary of the artery is partially structured within an axial distance  $L_0$  due to the presence of each stenosis.

Figure 1 presents a dimensionless view of the shape of the inside boundary of the arterial segment with multi-stenosis shown on  $(z, r)$ -plane in the absence of the catheter, where  $R$  is the radial coordinate of the inside boundary of the artery as function of the axial variable  $z$ . We made dimensionless all the involved axial distances by dividing them by the stenosis length  $L_0$ , so that the artery segment and the geometry in figure 1 are shown over a dimensionless distance  $L/L_0 = (3d + 2L_0)/L_0$  in the axial direction, and we set  $d = 0.5L_0$ , where  $d$  is segment of the artery that does not contain the stenosis. We also designate  $\delta$  to be the maximum height of each stenosis into the lumen, which occurs at particular locations in the axial direction. In particular, we refer to a location corresponding to a value very close to the maximum height  $\delta$  of the

stenosis as the critical height such as the location at a dimensional distance about  $z = d+L_0/2$  or  $z = 2d+ L_0/2$  from the considered origin of the coordinate system.

We now first non-dimensionalize the governing equations (1a-h) using  $U$ ,  $L_0$ ,  $R_0$ ,  $\delta$  and  $\mu_0 U L_0/\delta^2$  as scales for velocity, axial length, radial length, rate of radial change and pressure, respectively, where  $U$  is the maximum velocity for the unidirectional flow in a cylindrical annulus (White, 1991). Next, we follow Srivastava and Rastogi (2010) and simplify the dimensionless form of the governing equations (1a-h) under the reasonable conditions for mild stenosis with small  $\delta$  as compared to  $R_0$ , unidirectional flow assumption (White, 1991) where the axial velocity component dominates over the radial velocity component, and subjected to the assumptions that the inertial terms in the governing momentum equations (1a-b, d-e) are sufficiently small and  $Re(\delta/L_0) \ll 1$ , where  $Re = U L_0 \rho_f / \mu_0$  is the Reynolds number. Under these conditions and assumptions (Srivastava and Rastogi, 2010), the pressure is only a function of  $z$  and (1a-h) lead to simpler equations. The non-dimensional form of these simpler equations are given below using the same symbols for the variables as their dimensional ones for simplicity of notations

$$(1-C) dP/dz = [(1-C)/(1-mC)] [(1/r)(\partial/\partial r)(r\partial u_f/\partial r)] + CS \beta^2 (u_p - u_f), \quad (2a)$$

$$dP/dz = S\beta^2 (u_f - u_p), \quad S = 4.5[4 + 3(8C - 3C^2)^{0.5} + 3C]/(2-3C)^2, \quad (2b)$$

where  $\beta = \delta/a_0$ . The equations (2a-b) are subjected to the following no slip boundary conditions

$$u_f = 0 \text{ on } r=r_1 \text{ and } u_f = 0 \text{ on } r = R(z), \quad (2c)$$

which holds in the presence of the catheter, and

$$\partial u_f / \partial z = 0 \text{ at } r=0 \text{ and } u_f = 0 \text{ on } r=R(z) \quad (2d)$$

in the absence of the catheter.

Using (2b) for  $(u_f - u_p)$  in (2a) and integrating twice with respect to  $r$  and making use of the boundary conditions given in (2c), we find that in the presence of catheter

$$u_f = (-1/4)[(1-mC)/(1-C)](dP/dz) \{ (R^2 - r^2) + [(R^2 - r_1^2) l_n(r/R)] / l_n(R/r_1) \}, \quad (3a)$$

and the expression for the axial velocity for the red cells is then found from (2b) in terms of the axial velocity for the plasma in the form

$$u_p = u_f - [1/(S\beta^2)](dP/dz). \quad (3b)$$

In the absence of the catheter the results are found to be (3b) and

$$u_f = (1/4)[(1-mC)/(1-C)](dP/dz)(r^2 - R^2). \quad (3c)$$

Since both expressions for the axial velocity of plasma and red cells given by (3a-c) are in terms of the unknown pressure gradient ( $dP/dz$ ), we obtain expressions for the pressure gradient for both cases with or without catheter by assuming a prescribed volume flow rate in the annulus given by

$$Q=2\pi\int_{r_1}^R r[(1-C)u_f+ C u_p]dr. \quad (4)$$

Using (3a-c) in (4) and solving for the pressure gradient, we find

$$dP/dz = -\{Q/[(\pi/16)(R^2-r_1^2)]\}/\{[16C/(S\beta^2)]+2[(R^2-r_1^2)/(1-C)](1-mC)[(R^2+r_1^2)/(R^2-r_1^2)-1/\ln(R/r_1)]\}, \quad (5a)$$

which holds in the presence of the catheter, while in the absence of the catheter we have

$$dP/dz = -\{Q/[(\pi/16)R^2]\}/\{[16 C/(S\beta^2)]+2 R^2 [(1-mC)/(1-C)]\} \quad (5b)$$

The flow resistance, referred to as the impedance  $\lambda$ , is given by

$$\lambda = \Delta P/Q, \quad (6a)$$

where  $\Delta p$  is the pressure drop across the length  $L=1+2b$  for single stenosis case or  $L=2+3 b$  for multi stenosis given by

$$\Delta P= P(0)-P(L)=\int_0^L (dP/dz)dz \quad (6b)$$

and

$$b=d/L_0.$$

From (3a), we find the wall shear stress  $\tau_w$  to be

$$\tau_w = -\partial u_f / \partial r|_{r=R(z)} = -[R(1-mC)/(2-2C)](dP/dz) - [1/(4R)] [(1-mC)/(1-C)] (dP/dz) [(r_1^2 - R^2) / \ln(R/r_1)], \quad (7a)$$

for the case where the catheter is present in the artery, while in the absence of catheter we find from (3c) the following result:

$$\tau_w = -[R(1-mC)/(2-2 C)](dP/dz). \quad (7b)$$

The force  $F$ , referred to here as the integral of the shear stress over the surface of the artery from  $z = 0$  to  $z = L = 1+2b$  for the single stenosis case or  $z = L = 2+3b$  for the multi stenosis case is then given by

$$F=2\pi \int_0^L \tau_w dz. \quad (7c)$$

The values of the wall shear stress at different location can then be found from (7a)-(7b) for specific  $z$  value, and the surface integrated stress force  $F$  can be evaluated from (7c) for different parameter values in the presence or absence of the catheter.

### 3. Results and Discussion

We first calculated the inside radius for each of a number of cross-sectional areas within 2 or 3 mm intervals of a segment of about 26.7 mm along the axis of an actual human artery in the form of a circular cylindrical tube with mild stenosis, which were measured and recorded by Back et al. (1984). We then made these data of our calculated values for the inside radius of the artery dimensionless by dividing the value of each radius by the value of the radius  $R_0$  of the normal artery. Thus, we produced figure 1 for the shape  $R(z)$  of the artery versus the dimensionless  $z$  in the plane  $(r, z)$ . We made use of our generated data for  $R$  to carry out numerical calculation of various quantities, which were analyzed in the previous section. We make use of Simpson's Rule (Isaacson and Keller, 1966) to generate data for the integral quantities, such as impedance and the force due to the surface integrated stress, as well as numerical integration to generate data for the expressions of other quantities such as blood pressure gradient, plasma and red cell velocities and wall shear stress. For all the calculations, we set  $R_0$  (radius of normal artery) = 0.1 cm,  $L_0$  (stenosis length)=2.6 cm (Back et al., 1984),  $Q=1$ ,  $b=0.5$  and  $\beta=\delta/0.004$ , where  $\delta=(1-\text{minimum value of } R)$  (Back, 1994; Srivastava, 1996). We generated data for  $C=0.0, 0.1, 0.3, 0.5$ ;  $r_l=0.0, 0.1, 0.3, 0.5$ ;  $0 \leq z \leq 2$  for single stenosis case,  $0 \leq z \leq 3.5$  for multi stenosis case;  $r=0.0, 0.1, 0.3, 0.5$ .

Figures 2-5 present results for  $dP/dz$  (axial rate change of the blood pressure in the artery) versus the axial variable  $z$  in the presence or absence of the catheter. Figure 2 presents the pressure gradient versus  $z$  for the single stenosis case, hematocrit parameter=0.1 and for both in the absence or presence of the catheter with two different values of the catheter's radius. It can be seen from this figure that the blood pressure gradient is negative implying that the blood pressure force is in the direction of the positive  $z$ -axis. The blood pressure force does not vary with respect to the axial variable for the axial locations outside the stenosis zone. However, the magnitude of the blood pressure force increases with the stenosis effect in the stenosis zone. The magnitude of the pressure force also increases with the radius of the catheter. For example, for  $C = 0.1$  and at  $z = 1.04$ , which is at the critical height of the stenosis, this magnitude is a maximum and has the values of 22.05 and 47.10, respectively, for  $r_l = 0.1$  and 0.3. The effect due to the presence of the catheter is mainly to increase the magnitude of the axial rate of change of the blood pressure, which intensifies notably under the stenosis location. These results are physically reasonable since, for example, presence of both catheter and the stenosis zone, which reduces the cross sectional area for flow in the artery, can intensify the blood pressure force in the artery. This is due to the fact that the total volume flow rate is maintained at a fixed amount and, thus, smaller cross sectional area in the artery implies higher blood flow velocity, which can imply higher pressure driven force.

Figure 3 presents the pressure gradient versus  $z$  for single stenosis case,  $C = 0.5$  and several values of  $r_l = 0, 0.1, 0.3$  for cases with or without catheter. Comparing the results presented in



Figures 2-3, we find that the magnitude of the pressure gradient increases with the hematocrit parameter. For example, in the absence of the catheter and at the critical height with  $z = 1.04$  the magnitude of the pressure gradient is a maximum and has the values of 11.24 and 12.33 for the corresponding values of  $C = 0.1$  and 0.5, and in the presence of catheter for  $r_I = 0.1$  we have the values 22.05 and 24.17, respectively, at  $C = 0.1$  and 0.5. So, it appears that higher percentage of the red cells in the plasma can intensify the pressure driven force in the artery.

Figures 4 and 5 present pressure gradient versus  $z$  for multi stenosis case,  $r_I = 0, 0.1, 0.3$  and  $C = 0.1$  and 0.5, respectively. It can be seen that the magnitude of the blood pressure forces in the artery have now higher variations and intensification than those presented in Figures 2 and 3 for the single stenosis case, which are due to the presence of the multi stenosis as compared to those seen in Figures 2-3 for the single stenosis case.

Figures 6 and 7 present the impedance (flow resistance) versus the hematocrit in the presence or absence of the catheter and for single- and multi-stenosis cases, respectively. It can be seen from these figures that the impedance increases with the hematocrit, and the rate of increase of the impedance is higher either for very small hematocrit or relatively larger values of the hematocrit. The impedance also increases with the radius of the catheter. Thus, presence of the catheter increases the amount of flow resistance by the blood flow system. In addition, by comparing the results presented in these two figures, we find that presence of multi stenosis lead to notably higher values of the impedance for given values of the other parameters. These results indicate an inter-relationship between the amounts of blood flow resistance and the value of the radius of the catheter, which may only be present for a short period of time, for a given blood flow system with specific amounts of red cells in an artery and in the presence of single or multi stenosis.

Figures 8-11 present the axial velocity  $u_f$  of the blood plasma versus the axial variable or radial variable for the blood flow system with multi stenosis, for given value of the hematocrit parameter and in the presence or absence of the catheter. Our additional collected data for the corresponding red cell velocity  $u_p$  indicate that for given values of the parameters, the values of the plasma velocity are equal to red cell velocity within an order accuracy of order ( $10^{-4}$ ), and, thus, the results presented in this section for the plasma velocity are also applicable for red cell velocity. Our generated data indicated that maximum value of  $u_p$  is very slightly larger than maximum value of  $u_f$  by a very small quantity of order about 0.0001 for both single and multi stenosis cases. We also calculated the corresponding results for the plasma velocity in the single stenosis case, and we found that values of the plasma velocity for the multi stenosis case are higher than the corresponding ones for the single stenosis case.

Figures 8-9 present plasma velocity versus the axial variable for  $r = 0.5$ ,  $C = 0.1$  and 0.5, respectively, and for the cases with or without the catheter. It can be seen from these figures that the plasma velocity is positive, which makes sense since the blood pressure force is in the positive direction of the axis of the artery system. The plasma velocity is constant outside the stenosis zone, while it is variable in the stenosis zone and its magnitude increases with the stenosis effect. This result is reasonable since as we explained before, higher stenosis effect reduces the cross sectional area of inside artery leading to higher blood plasma velocity. The plasma velocity also increases with the catheter radius, which is reasonable since higher catheter radius decreases the annulus gap leading to higher axial velocity of the fluid. The plasma

velocity also increases with the hematocrit parameter. Presence of the catheter can be seen to increase the plasma velocity, while such velocity diminishes very close to the catheter boundary.

Figures 10-11 present plasma velocity versus the radial variable for  $z=2.5$ ,  $C=0.5$ , and for cases without and with the catheter, respectively. The results shown in Figure 10 which presents the plasma velocity in the artery with on catheter, indicate that plasma velocity decreases with increasing the radial variable and its maximum value is at the center of the artery. The rate of decrease of the plasma speed is higher close to the upper values of  $r$  and close to the stenosis zone. It should also be noted from the parabolic shape of the plasma velocity in this figure, which is based on (3c), and the corresponding velocity profile in Hagen-Poiseuille flow (White, 1991) that their expressions differ only by additional constant coefficient  $(1-mC)/(1-C)$  which is in (3c). Figure 11 presents results for the plasma velocity versus the radial variable and in the presence of the catheter. It can be seen from this figure that the plasma velocity satisfies its zero no-slip conditions at the two boundaries of the catheterized artery system, while it has a maximum value at some location in the annulus away from the boundaries. Comparing the results shown in Figures 10-11, we find that the presence of the catheter appears to decrease radially the magnitude of the plasma velocity.

Figure 12 presents wall shear stress versus the axial variable for the multi stenosis and for two different values 0.1 and 0.5 of the hematocrit parameter in the absence or presence of the catheter. It can be seen from this figure that the wall shear stress is higher for the hematocrit parameter =0.5 in the presence of the catheter, while dependence of the shear stress on the hematocrit is negligible in the absence of the catheter. This result indicates that joint effects of the catheter and the presence of not too small percentage of red cells in the blood reinforce the effect on the wall shear stress since presence of catheter also increases the value of the wall shear stress. The wall shear stress is constant in the regions outside from the stenosis zones, while the shear stress has notable high values in the stenosis zones and its rate of increase becomes significantly higher with increase in the severity of the stenosis. The value of the shear stress is positive which indicates that such stress is acted by the blood flow on the artery.

Figures 13 and 14 present the surface integrated wall shear stress on the artery versus the hematocrit parameter for the multi stenosis case and in the absence (Figure 13) or presence (Figure 14) of the catheter. It can be seen from these figures that for sufficiently small values of the hematocrit, this force decreases with increasing the hematocrit, while the surface integrated wall shear stress increases with the hematocrit if the volume fraction density of red cells in the plasma is not too small. In addition, the value of such force is higher in the presence of the catheter. These figures also show that the shear stress on the wall of the artery is very similar without red blood cells as with 100% presence of red blood cells, but the shear stress is lower with intermediate values of hematocrit. This result indicates that for intermediate values of the hematocrit, there is shear thinning near the wall which reduces viscosity and consequently the stress on the wall.

About comparison of the present results to those of related studies by other authors, it should be noted that no other studies have been reported so far that take into account experimental data of the type due to Back et al. (1984) for the shape of the stenosis in an arterial blood flow system. However, Srivastava and Rastogi (2010) investigated two-phase blood flow in a catheterized

artery and in the presence of a single stenosis whose shape was assumed analytically in the form of a simple mathematical function. They calculated different quantities including impedance and wall shear stress. They found, in particular, that impedance increases with  $C$ , and this variation and its rate of increase with respect to  $C$  were qualitatively similar to those predicted in the present study for the single stenosis, but the quantitative values of the impedance were smaller than those of the present results. In addition, values of the impedance in the absence of the catheter were smaller than those in the presence of the catheter, which are consistent with the present results as well. Their results about wall shear stress versus  $z$  indicated that wall shear is non-constant throughout the investigated artery segment, first increases with  $z$ , reaches a maximum value at some intermediate value of the axial variable and then decreases with increasing  $z$ , while the present results indicated that the wall shear stress is a constant in the sections of the artery which are outside the stenosis zone. In addition, their results indicated that the wall shear stress increases with  $r_l$  or  $C$ , which generally agree with the present results.

Riahi et al. (2011) studied single-phase arterial blood flow in the absence of a catheter but in the presence of an overlapping stenosis whose shape was based on an assumed analytical form. They calculated several quantities including the axial velocity, impedance and wall shear stress. Their results about axial blood velocity versus  $z$  indicated that axial velocity was non-constant only in the section of the stenosis zone, but the form of the variation of the axial velocity with respect to  $z$  in the stenosis zone was different from that in the present study. Their results about impedance versus the hematocrit parameter indicated a linear increase of impedance with respect to the hematocrit parameter, which is somewhat different from the present results that show a nonlinear increase. In summary, we should note that, aside from the general agreement, a few differences between the results of the other studies and those of the present one that were described above are expected due to the differences on at least the shape of the stenosis with either single or multiphase type flow that were existed between the present model and those investigated by other authors. In addition, we should also state that the present model also has its own limitations. It is valid only for mild stenosis cases, unidirectional flow approximation, sufficiently small Reynolds number flow with negligible inertial terms in the momentum equations.

#### 4. Conclusion

We investigated the arterial two-phase blood flow with or without a catheter and in the presence of single or multiple stenosis. Our modeling for the stenosis was based on the available experimental data for a human's artery with stenosis. We calculated important quantities, such as the pressure gradient force, the plasma velocity, the impedance, the wall shear stress and the force due to the surface integrated wall shear stress in the artery which contained either a single or multiple stenosis and in the presence or absence of a catheter. We found, in particular, that the magnitudes of all those stated quantities can increase with the hematocrit of the blood, with the exception of the result that the force due to the surface integrated wall shear stress decreases slightly with increasing the hematocrit if the percentage of the red cell in the plasma is too small. We also determined that the impedance and the force due to the surface integrated wall shear stress are stronger in the presence of multi stenosis, and the presence of the catheter can increase

the values of the blood velocity, magnitude of the pressure gradient, the wall shear stress, the force due to the surface integrated wall shear stress and the impedance. These results could be relevant and of interest for understanding the biomechanical conditions for the blood flow in narrow arteries, which contain either single or multi stenosis.

The extension of the present paper to the cases of two-phase arterial flow with or without an inserted catheter with included effects of heat transfer and gravity and in the presence of multi stenosis will be investigated by the authors in near future. Another important extension of the present study can be for the medically more realistic finite systems with cases conforming to the medically generated data in order to identify the components of arterial blood flow diseases which could be used to improve the health conditions of the corresponding patients.

### ***Acknowledgement***

*The authors would like to thank the three reviewers for their useful comments and suggestions that improved the content of the paper.*

## **REFERENCES**

- Back, L. H., Cho, Y. I., Crawford, D. W. and Cuffel, R. F. (1984). Effect of mild atherosclerosis on flow resistance in a coronary artery casting of man, Transactions of the ASME, Vol. 106, pp. 48-53.
- Back, L. H. (1994). Estimated mean flow resistance during coronary artery catheterization, Journal of Biomechanics, Vol. 27, pp.169-175.
- Back, L. H., Kwack, E. Y. and Back, M. R. (1996). Flow rate-pressure drop relation to coronary angioplasty: Catheter obstruction effect, Journal of Biomedical Engineering, Vol. 118, pp. 83-89.
- Batchelor, G. (1970). An Introduction to Fluid Dynamics, Cambridge University Press, UK.
- Charm, S. E. and Kurland, G. S. (1974). Blood Flow and Microcirculation, John Wiley and Sons, Inc., New York.
- Isaacson, E. and Keller, H. B. (1966). Analysis of Numerical Methods, John Willey and Sons, Inc., New York.
- Kanai, H., Lizuka, M. and Sakamotos, K. (1970). One of the problems in the measurement of blood pressure by catheterization: Wave reflection at the tip of catheter, Med. Biol. Engr., Vol. 28, pp. 483-496.
- Mishra, B. K. (2003). A mathematical model for the analysis of blood flow in arterial stenosis, The Mathematics Education, Vol. 37, pp. 176-181.
- Mishra, B. K. and Panda, T. C. (2005). Non-Newtonian model of blood flow through an arterial stenosis, Acta Ciencia Indica, Vol. 31, No. M(2), pp. 341-348.
- Riahi, D. N., Roy, R. and Cavazos, S. (2011). On arterial blood flow in presence of an overlapping stenosis, Mathematical and Computer Modelling, Vol. 54, pp. 2999-3006.
- Smali, O., Packirisamy, M., Stiharu, I. and Rakheja, S. (2006). Modeling of blood flow through multi-stenosis, IEEE ISIE, July 9-12, 2006, Montreal, Canada, pp. 3400-3403.

- Srivastava, V. P. (1996). Two-phase model of blood flow through stenosed tubes in the presence of a peripheral layer: Applications, *Journal of Biomechanics*, Vol. 29, pp. 1377-1382.
- Srivastava, L. M. and Srivastava, V. P. (1983). On two-phase model of pulsatile blood flow with entrance effects, *Bio-Rheology*, Vol. 20, pp. 761-777.
- Srivastava, V. P. and Srivastava, R. (2009). Particulate suspension blood flow through a narrow catheterized artery, *Computers and Mathematics with Applications*, Vol. 58, pp. 227-238.
- Srivastava, V. P., Rastogi, R. and Mishra, S. (2010). Non-Newtonian arterial blood flow through an overlapping stenosis, *Applications and Applied Math: An Int. Journal*, Vol. 5, No. 1, pp. 225-238.
- Srivastava, V. P. and Rastogi, R. (2010). Blood flow through a stenosed catheterized artery: Effects of hematocrit and stenosis shape, *Computer and Mathematics with Applications*, Vol. 59, pp. 1377-1385.
- Tam, C. K. W. (1969). The drag on a cloud of spherical particles in low Reynolds number flows, *Journal of Fluid Mechanics*, Vol. 38, pp. 537-546.
- Venkateswarlu, K. and Rao, J. A. (2004). Numerical solution of unsteady blood flow through an indented tube with atherosclerosis, *Indian Journal of Biochemistry and Biophysics*, Vol. 41, pp. 241-245.
- White, F. M. (1991). *Viscous Fluid Flow*, Second Edition, McGraw-Hill, Inc., New York.
- Young, D. F. and Tsai, F. Y. (1973). Flow characteristics in model of arterial stenosis-steady flow, *J. Biomechanics*, Vol. 6, pp. 395-410.

## FIGURES

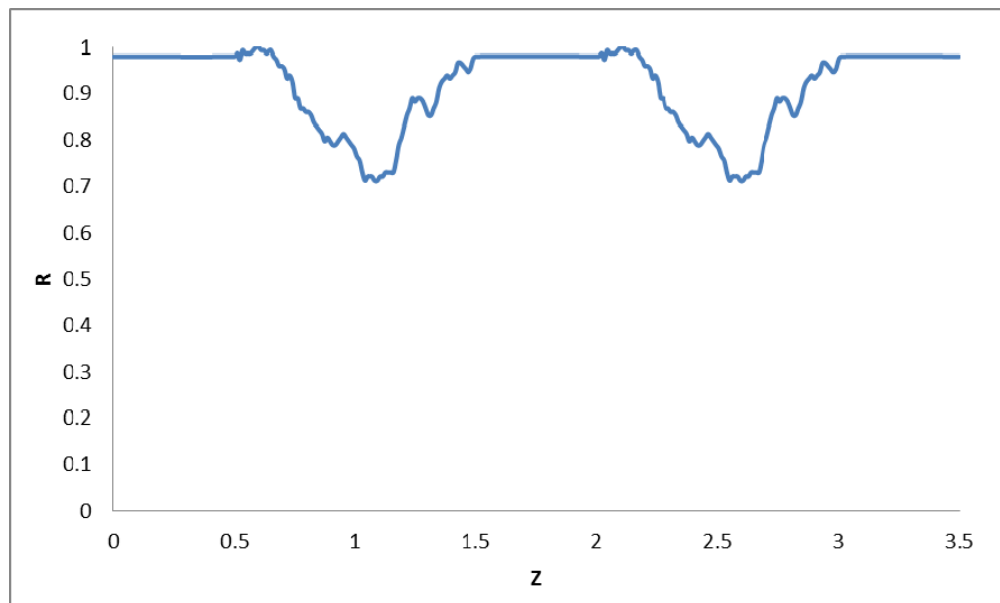


**Figure 1.** Plane view of the shape  $R$  for boundary of arterial segment versus axial variable  $z$

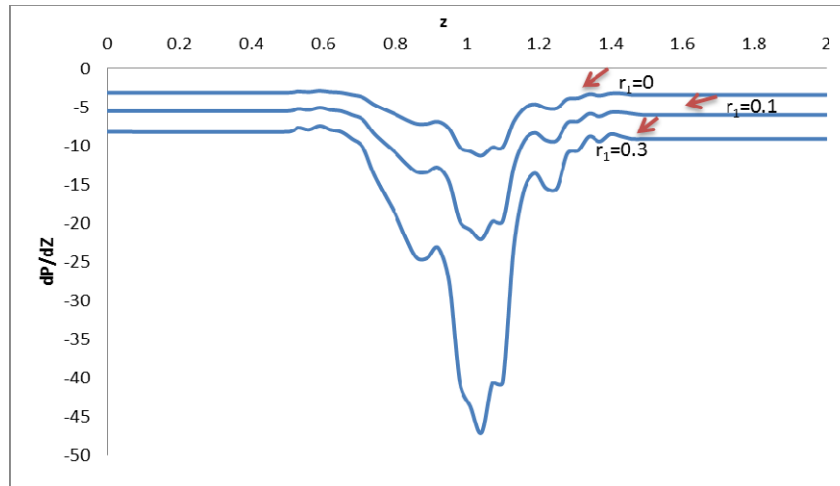


**Figure 2.** Pressure gradient versus  $z$  for single stenosis case,  $C=0.1$  & 3 values of  $r_1$

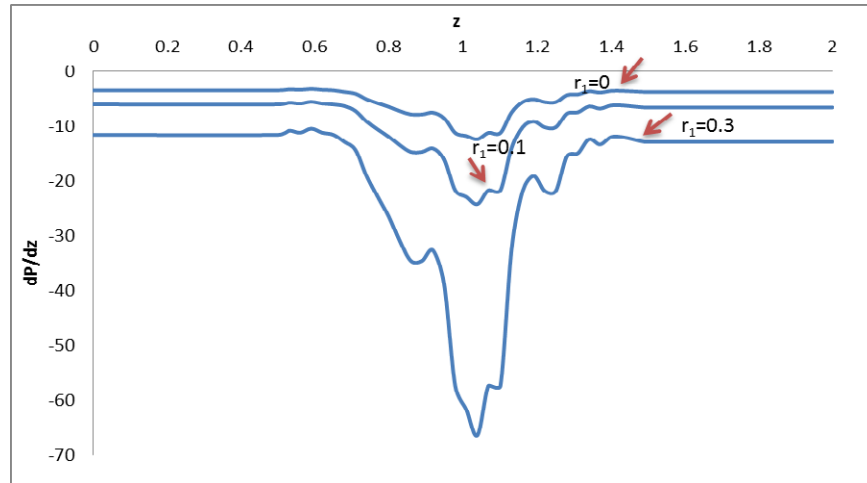


**Figure 3.** Pressure gradient versus  $z$  for single stenosis case,  $C=0.5$  & 3 values of  $r_1$

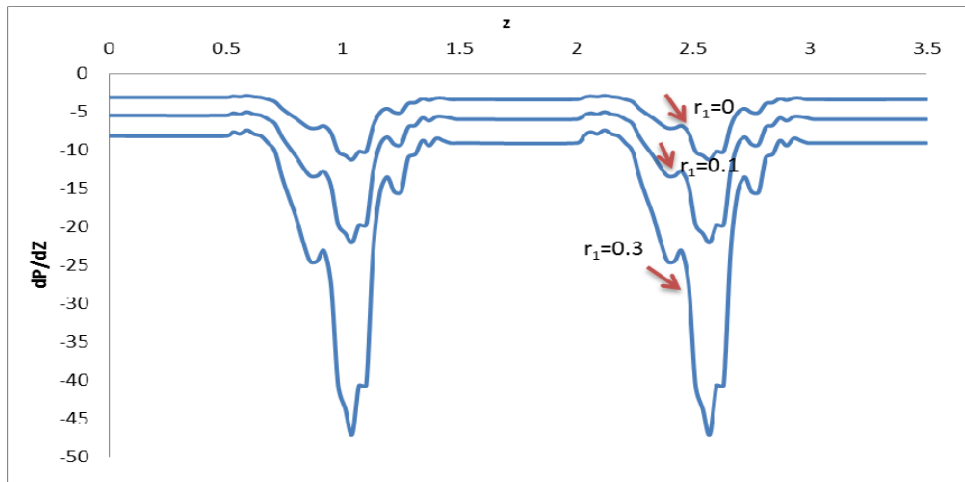


**Figure 4.** Pressure gradient versus  $z$  for multi stenosis case,  $C=0.1$  & 3 values of  $r_1$

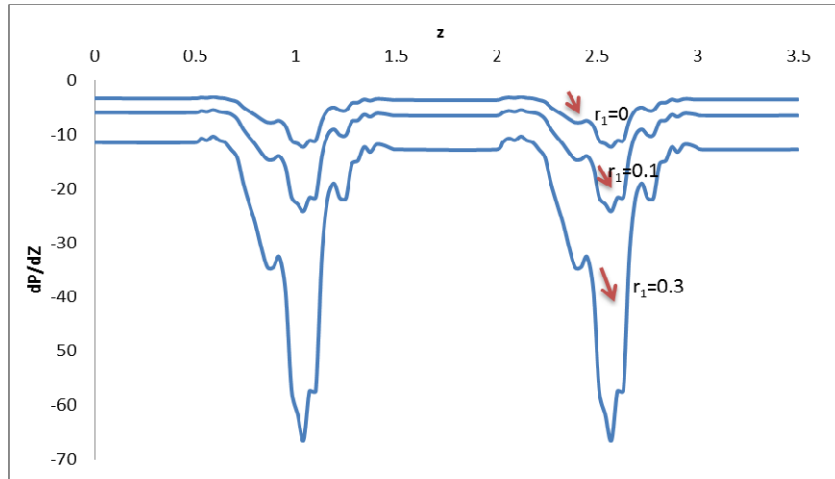


**Figure 5.** Pressure gradient versus  $z$  for multi stenosis case,  $C=0.5$  & 3 values of  $r_1$

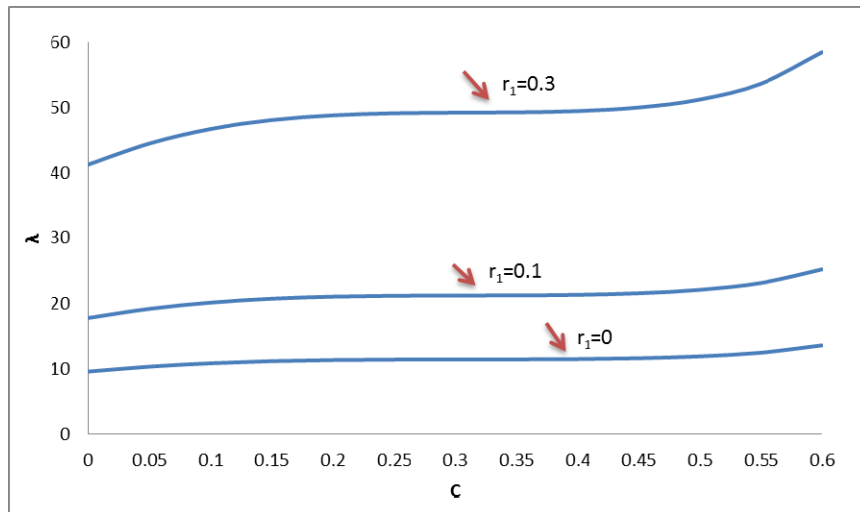


**Figure 6.** Impedance  $\lambda$  versus  $C$  for single stenosis case & 3 values of  $r_1$

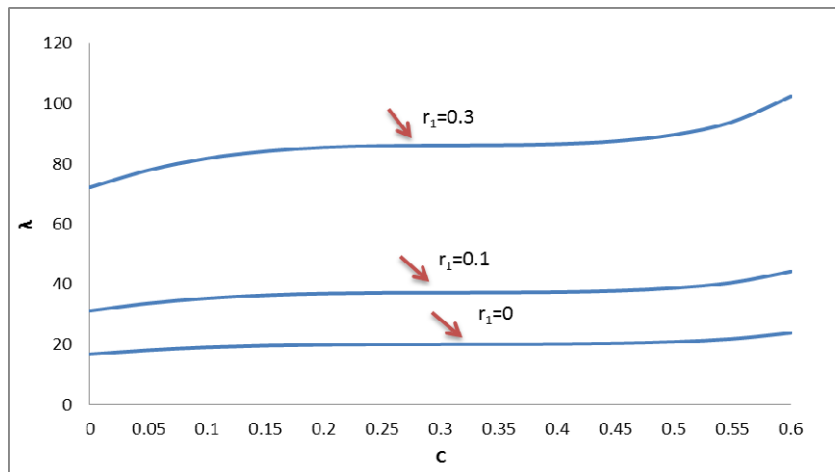


**Figure 7.** Impedance  $\lambda$  versus  $C$  for multi stenosis case & 3 values of  $r_1$

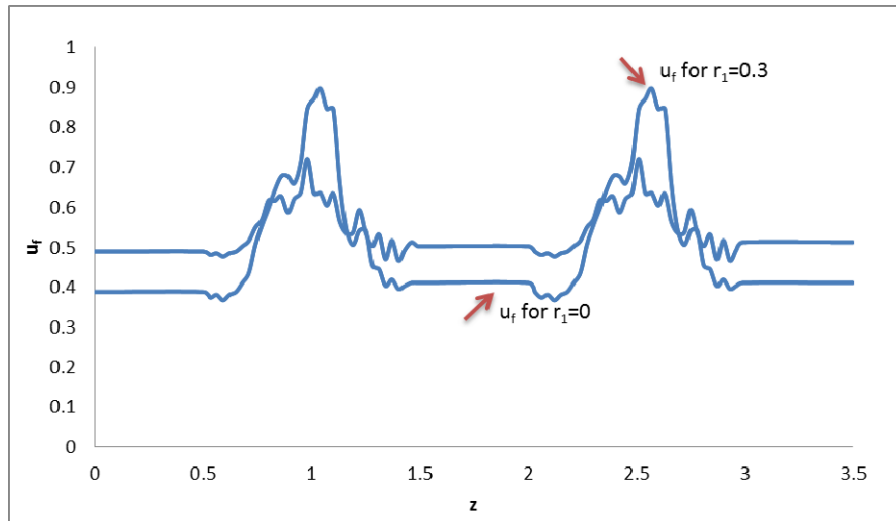


**Figure 8.** Plasma velocity versus  $z$  for multi stenosis case,  $r=0.5$ ,  $C=0.1$  & two values of  $r_1$

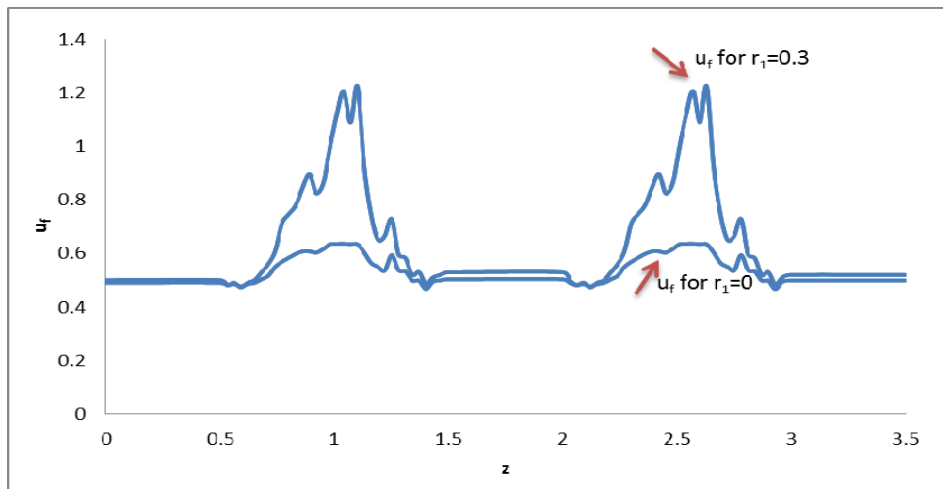


**Figure 9.** Plasma velocity versus  $z$  for multi stenosis case,  $r=0.5$ ,  $C=0.5$  & 2 values of  $r_1$

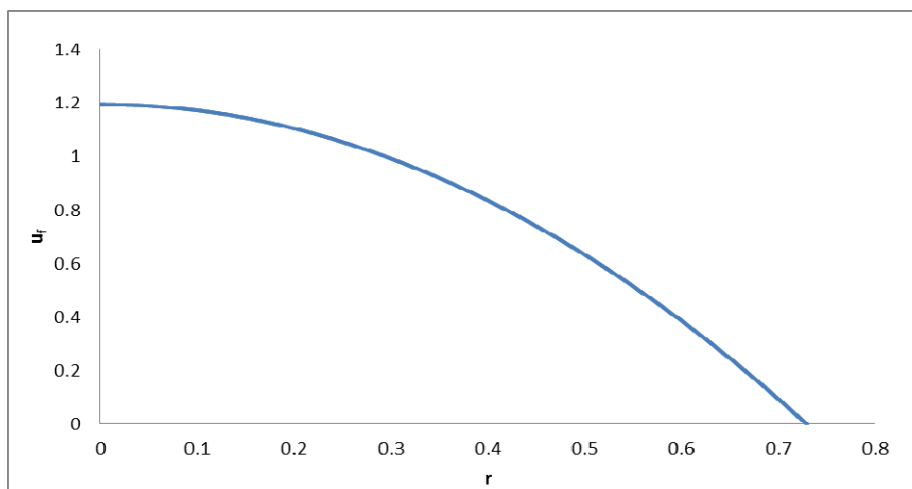


**Figure 10.** Plasma velocity versus radial variable  $r$  for multi stenosis case,  $z=2.5$ ,  $C=0.5$ ,  $r_1=0$



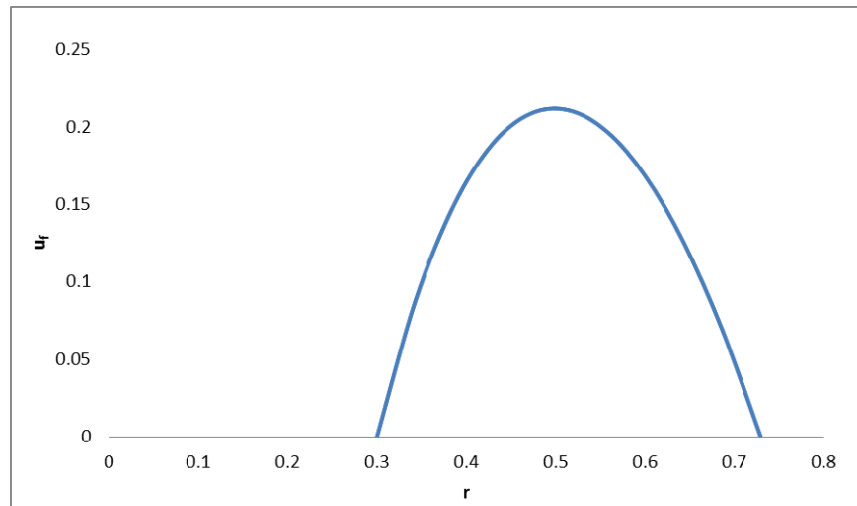


**Figure 11.** Plasma velocity versus  $r$  for multi stenosis,  $z=2.5$ ,  $C=0.5$ ,  $r_1=0.3$

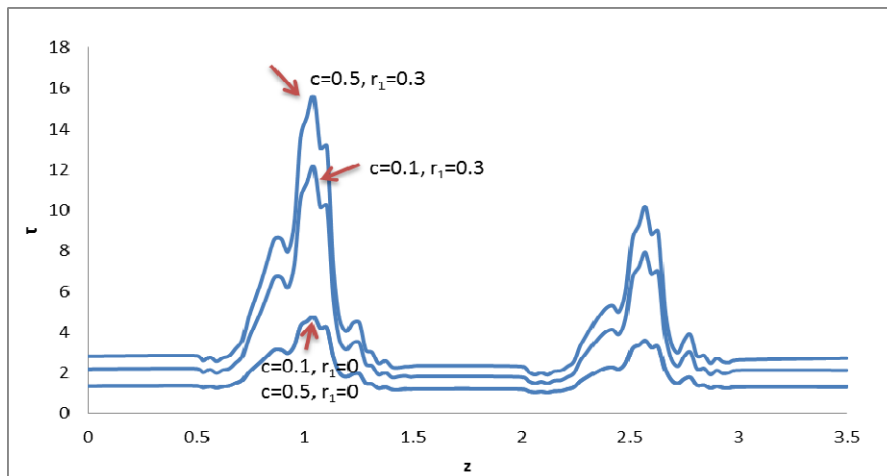


**Figure 12.** Wall shear stress versus  $z$  for two different values of  $C$  and  $r_1$

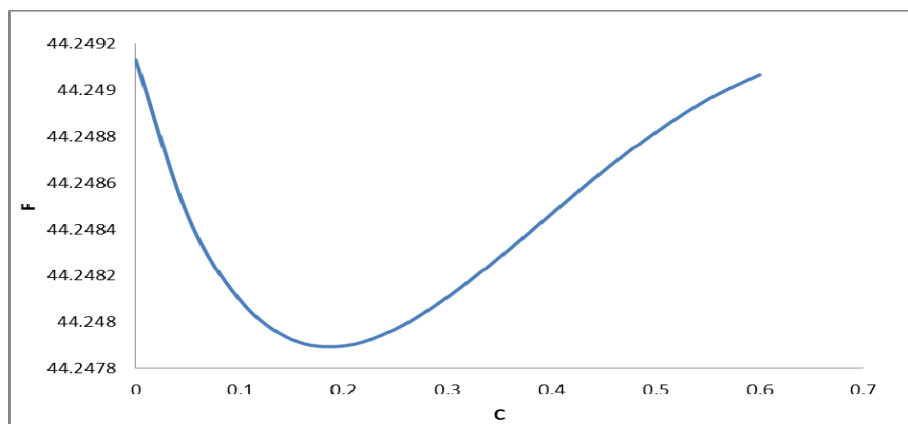


**Figure 13.** Surface integrated shear stress  $F$  versus  $C$  for  $r_1=0$

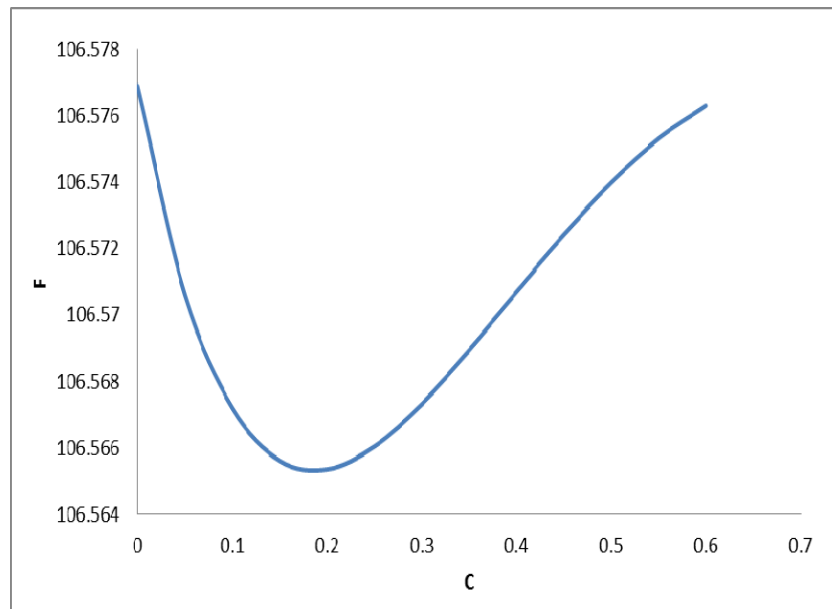


**Figure 14.** Surface integrated shear stress  $F$  versus  $C$  for  $r_l=0.3$